Available online at www.sciencedirect.com
SCIENCE DIRECT®
Bioelectrochemistry 63 (2004) 137–147
Bioelectrochemistry
www.elsevier.com/locate/bioelechem

Spectroelectrochemical studies of bilayers of phospholipids in gel and liquid state on Au(111) electrode surface

Izabella Zawisza, Xiaomin Bin, Jacek Lipkowski*

Department of Chemistry and Biochemistry, University of Guelph, Guelph, Ontario, Canada N1G2W1

Received 7 October 2003; received in revised form 28 November 2003; accepted 3 December 2003

Abstract

Differential capacity, chronocoulometry and Polarization Modulation Fourier Transform Infrared Reflection Absorption Spectroscopy (PM FTIRRAS) were employed to investigate spreading of small unilamellar vesicles (SUVs) of DOPC and DMPC onto a Au(111) electrode surface. The electrochemical experiments demonstrated that vesicles fuse onto the electrode surface and at $E > -0.5$V (SSCE) or at charge densities $-10 < \sigma_M < 5$ μC cm^{-2} to form defected bilayers, directly in contact with the metal surface. The analysis of PM FTIRRA spectra in the CH stretching region showed that the DOPC bilayer is in the liquid crystalline state while the bilayer of DMPC is in the gel or in the ripple phase. The spectra were also used to determine the tilt of the acyl chains in the bilayer of DMPC as a function of the electrode potential. At $E < -0.5$ V (SSCE), where the bilayer is detached from the metal surface, the chains are tilted at $\sim 29°$ with respect to surface normal. When the bilayer is adsorbed at the metal surface at $E > -0.5$ V (SSCE), the tilt angle increases to $\sim 42°$. The increase of the tilt angle is discussed in terms of a change in the packing of the polar head of the phospholipids molecules in the bilayer adsorbed at the electrode surface.

Keywords: Phospholipid bilayer; Differential capacity; Electrode; Polarization Modulation Fourier Transform Infrared Reflection Absorption Spectroscopy (PM FTIRRAS)

1. Introduction

Biommimetic studies require an artificial membrane existing in the liquid crystalline state containing aqueous solution on both sides of the membrane, capable to incorporate in its structure other molecules such as cholesterol, sugars and proteins [1–3]. The bilayers of lipids can be deposited onto a solid substrate using different methods: Langmuir–Blodgett, Langmuir–Schaeffer (known also as the horizontal touch method), self-assembly or spreading of vesicles [2–6]. The Langmuir–Blodgett method gives well-ordered lipid monolayers, but the problem arises when one attempts to transfer the second layer [1,4]. A combination of the Langmuir–Blodgett and the Langmuir–Scheaffer methods was found to be the best strategy to deposit lipid bilayers on solid substrates [1,4]. Lipids can also be chemically modified in order to obtain bilayers tethered to the solid support [5–7].

In order to investigate trans-membrane proteins, significant efforts have been made to obtain bilayers containing aqueous solution on both sides of the membrane [1,3]. It has been shown that spreading of small unilamellar vesicles (SUVs) on hydrophilic substrates (mica or glass) results in formation of a bilayer suspended on a thin cushion of water [6,8] that is usually 1.0–1.5-nm thick [9]. Another strategy relies on the use of thio-derivatives that are hydrophilic and can accumulate water into the monolayer tethered to the solid support. The bilayer is then formed by fusing SUVs onto the thiol-modified solid surface [7,10–12].

In order to study voltage gated phenomena, it is convenient to deposit a model biomimetic membrane onto a conductive substrate. For that purpose, monolayers [13–15] and bilayers [2,8,15–21] have been deposited on metal electrode surfaces such as gold or mercury. By fusion of SUVs, a phospholipid bilayer may be deposited either onto a clean metal surface [8,18–20] or onto a

* Corresponding author. Tel.: +1-519-8244-120; fax: +1-519-766-1499.
E-mail address: lipkowski@chembio.uoguelph.ca (J. Lipkowski).

1567-5394/$ - see front matter © 2004 Elsevier B.V. All rights reserved.
doi:10.1016/j.bioelechem.2003.12.004

surface modified by a monolayer of a hydrophilic thiol [2,16,17,21]. The membrane directly deposited at the metal may be used as a matrix to investigate proteins adsorbed at the membrane or imbedded into the leaflet facing the solution. The membranes supported on a tethered hydrophilic monolayer may be used to study transmembrane proteins. Electrode is an important substrate because the biomimetic membrane supported at the electrode surface may be exposed to electric fields, comparable in the magnitude to the fields to which the natural biological membranes are exposed [22].

Most of the past studies of membranes supported at an electrode surface involved measurements of average properties such as electrode capacity, charge density or impedance. Less is known how the field applied to the membrane supported at the electrode surface affects the membrane structure, orientation and conformation of the phospholipid molecules. We have recently developed in situ Polarization Modulation Fourier Transform Infrared Reflection Absorption Spectroscopy (PM FTIRRAS) [23] and have employed this technique to investigate field-driven transformations of DMPC [18,20] and DOPC [19] bilayers at a gold electrode surface.

The objective of this paper is to demonstrate the power of the in situ PM IRRAS to investigate the field-driven changes in the orientation and conformation of the acyl chains in the DMPC and DOPC bilayers supported at the gold electrode surface. The DMPC has two fully saturated 14-carbon-atom-long acyl chains that consist of 12 methylene (CH_2), one methyl (CH_3) and one ester carbonyl group. The acyl chains of DOPC are 18 carbon atoms long, each. They have a double bond at the nine's carbon atom position and therefore they are built of 14 methylene, one methyl and one ester carbonyl group. Since we will investigate the properties of methylene and methyl vibrations in these molecules, it is important to emphasize that the number of CH_3 groups in these two molecules is identical and the difference between numbers of CH_2 groups is small.

Due to the presence of the double bond, the physical properties of DOPC bilayer are distinctly different than the properties of a bilayer of DMPC. In vesicles, the gel–liquid crystal phase transition for DOPC is observed at −22 °C [24] while for DMPC it occurs at 24 °C [25]. Our experiments were performed at the temperature of ~20 °C. Hence, the film of DOPC was in the liquid crystalline state while the bilayer of DMPC was in the gel state. Herein, we will demonstrate that the in situ PM FTIRRA spectroscopy is a unique tool to investigate the physical state of the bilayer deposited at the electrode surface and to determine the potential-driven changes in the orientation and conformation of the acyl chains of the phospholipids molecules. The Au(111) electrode was employed in these studies because it has an energetically uniform surface and a broad range of potentials where it displays an ideally polarizable behaviour. In the discussion of the results, we will use information concerning structure of the bilayer determined from neutron reflectivity experiments described in an earlier publication [26].

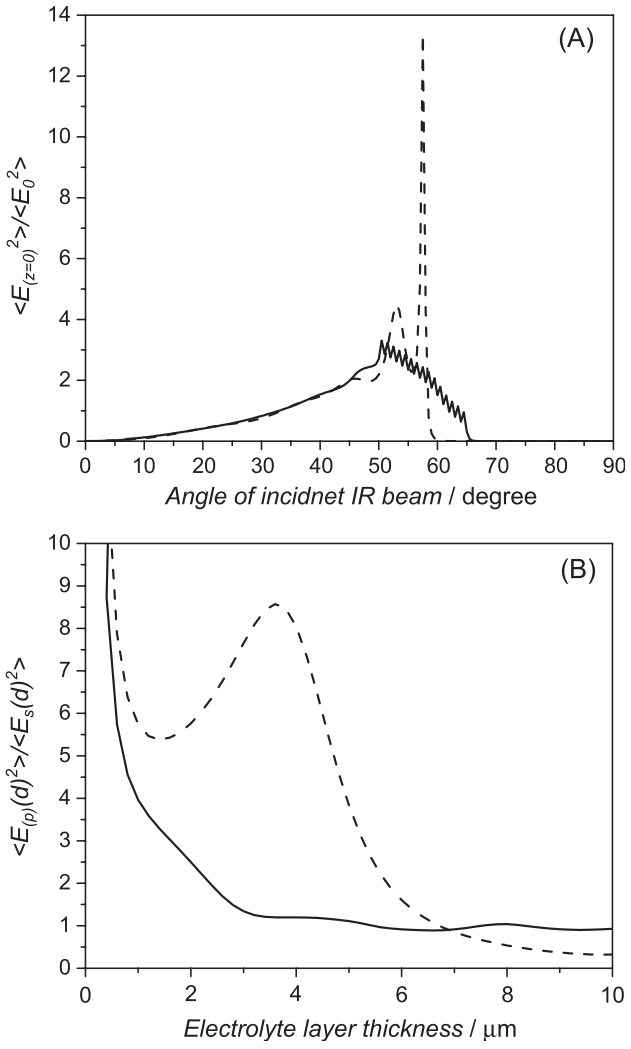

Fig. 1. (A) Time averaged mean squared electric fields of the p-polarized photon (frequency 2900 cm^{-1}) at the gold electrode surface plotted as a function of the angle of incidence in a three phase system, BaF_2/D_2O/Au; (dashed line)-parallel beam, (solid line) convergent beam with a 5° angle of convergence. The thickness of the D_2O layer 5.8 μm. (B) Ratio of the time and distance averaged mean square electric fields for p- and s-polarized photons plotted as a function of the thickness of the thin layer of D_2O in the three phase system BaF_2/D_2O/Au, for 53° angle of incidence and 2900 cm^{-1} photon frequency; (dashed line)-parallel beam, (solid line) convergent beam with a 5° angle of convergence.

2. Experimental

2.1. Reagents, solutions and electrodes

A 0.05 M NaF (EM Industries, Suprapur) solution was used as the supporting electrolyte. All aqueous solutions were prepared from ultra-pure water, purified by a Milli-Q UV Plus® (>18.2 MΩ cm) water system. Some IR experi-

ments were performed in deuterated water solutions (D_2O, Cambridge Isotope Laboratories, Cambridge, MA, USA). All electrolyte solutions were de-aerated by purging with argon (BOC Gases Inc.) for at least 20 min prior to starting the measurements. Argon was allowed to flow over the solution at all times. The gold(111) single crystal electrodes used in the electrochemical and the infrared experiments were grown, oriented, cut and polished in our laboratory. Prior to the experiments, the gold electrodes were cleaned by flame annealing and quenched with ultrapure water. A coil made of either Pt wire or Pt foil served as counter electrodes in the electrochemical and PM-IRRAS measurements, respectively. A saturated calomel electrode (SCE) was used as the reference electrode in the electrochemical experiments and a Ag/AgCl/3 M KCl (SSCE) reference electrode ($E = -40$ mV vs. the SCE) was used in IRRAS measurements. In this paper, all potentials are reported on the SSCE scale. Di-oleolyl phosphatidyl choline (DOPC, di-oleoyl lecithin) was purchased from Nutfield Nurseries, UK and dimyristoylphosphatidylcholine (DMPC) form Sigma and used without further purification. All measurements were carried out at room temperature (20 ± 2 °C). The procedure described by Barenholdz et al. [27] was used to prepare SUVs. The final concentration of phospholipids in the investigated solution was ca. 10^{-4} mol l^{-1}.

2.2. Electrochemical measurements

All electrochemical measurements were carried out in an all-glass three-electrode cell using the working electrode in the hanging meniscus configuration [28]. The cyclic voltammetry curves were recorded at a scan rate of 20 mV s^{-1}. The differential capacity curves were determined using a scan rate of 5 mV s^{-1} and an ac perturbation of 25-Hz frequency and 5-mV r.m.s. amplitude. A computer-controlled system, consisting of a HEKA potentiostat/galvanostat PG 490, a HEKA scan generator ESG310 (Lambrecht/Pfalz, Germany) and a 7265 DSP lock-in amplifier (EG&G Instruments, CA) was employed to perform electrochemical experiments. All data were acquired via a plug-in acquisition board (RC Electronics, CA) and in-house software. The differential capacity curves were calculated from the in-phase and the out-of-phase components of the ac current using a series RC equivalent circuit.

Chronocoulometry was used to determine the charge density at the electrode surface. The gold electrode was held at a base potential $E_b = -800$ mV for 30 s. Then the potential was stepped to a variable potential of interest, E_f, where the electrode was held for a time t_f of 70 s for DOPC and 180 s for DMPC bilayers. Stirring of the solution achieved in a complete spreading of vesicles at the electrode surface. A potential step to the desorption potential $E_{des} = -1.20$ $V_{Ag/AgCl}$ was then applied. The current transient was recorded during 200 ms and the potential was stepped back to E_b. The stirring was interrupted 10 s before the potential step from E_f to E_{des} was applied. The integration of the current transients gives the difference between charge densities at potentials E_f and E_{des}. Similar experiments were performed at the electrode in a solution without the vesicles. The absolute charge densities were then calculated using the independently determined potential of zero charge, $E_{pzc} = 310$ mV vs. Ag/AgCl, and the procedure described in Ref. [29].

2.3. Spectra collection and processing

The Nicolet, Nexus 870 (Madison, WI) spectrometer, equipped with an external tabletop optical mount, High D* MCT-A detector, photoelastic modulator (Hinds Instruments PM-90 with II/ZS50 ZnSe 50-kHz optical head, Hillsboro, OR) and demodulator (GWC Instruments Synchronous Sampling demodulator, Madison, WI) was used to perform PM FTIRRAS experiments. The spectra were acquired using in-house software, an Omnic macro and digital-to-analog converter (Omega, Stamford, CT) to control the potentiostat (HEKA PG285, Lambrecht/Pfalz, Germany) and to collect spectra. The IR window was a BaF_2 1″ equilateral prism (Janos Technology, Townshend, VT). Prior to the experiment, the window was washed in water and methanol and then cleaned for 10 min in an ozone chamber (UVO-cleaner, Jelight, Irvine, CA). When the spectroelectrochemical cell was assembled, vesicles prepared in D_2O were injected into the cell. After 1 h the phospholipids bilayer was formed on the Au(111) electrode surface. The WE was set at a starting potential $E = -1.00$ V vs. the Ag/AgCl reference electrode and spectra were collected at a series of potentials, which were programmed as a cyclic sequence of steps whose amplitude was progressively increased using 0.05, 0.1 or 0.2 V potential increments. In total, 20 cycles of 400 scans each were performed to give 8000 scans at every applied potential. The instrumental resolution was 2 cm^{-1}. At the end of the measurement, the blocks of scans were individually checked for anomalies, using in-house software, before averaging.

Measurements of IR spectra were carried out with the PEM set for half-wave retardation at 2900 cm^{-1} for the CH stretching region. A 2400–3200 cm^{-1} band-pass filter was employed. The intensity of reflected IR beam is the function of angle of incident light and the thickness of the electrolyte layer. In order to obtain highest intensity of p-polarized light, caring information on the species adsorbed on the electrode surface Fresnel equations were solved for the stratified medium: $BaF_2/D_2O/Au$ as the function of angle of incident beam and the thickness of electrolyte (Fig. 1). For the wave number of 2900 cm^{-1}, highest intensity of p-polarized light was obtained for the angle of incident light set to 53°. The electrolyte thickness between electrode and prism was ca. 5.8 μm, giving comparable intensities of p- and s-polarized light at the electrode

surface. In this way, we were able to remove absorbance originating from vesicles dissolved in the electrolyte solution. The thickness of the thin layer was determined by comparing the experimental reflectivity spectrum of the thin layer cell, attenuated due to the layer of solvent between the electrode and the IR window, to the reflectivity curve calculated from the optical constants of the cell constituents, as described in Ref. [30].

The demodulation technique developed in Corn's laboratory [31,32] was used in this work. After demodulation, two signals were measured: (i) the averaged intensity $I_A(\omega)$ and (ii) the intensity difference $I_D(\omega)$. The two signals have to be corrected for the PEM response functions. A procedure which is a modified version of a method described earlier in Ref. [33] was employed to calculate the PEM response functions. The details of the calculations and the calculated PEM response functions are described in Ref. [23]. The signals $I_A(\omega)$ and $I_D(\omega)$ have to be corrected further for the difference between optical throughputs of the optical set-up for p- and s-polarized light [23,33]. The ratio of the throughputs of the optical set-up for p- and s-polarized light was equal to 1.06 [23].

Finally, when in situ experiments are performed in a thin layer cell that contains electrolyte, the measured spectrum has a background due to the absorption of the IR beam by the aqueous solution in the thin layer. To correct the spectra for the background, a baseline was built for each spectrum using a spline interpolation technique [23]. The same data points were used to build the spline for all the spectra. When all these corrections are introduced, the background corrected spectrum plots ΔS, which is proportional to absorbance A of the adsorbed molecules:

$$\Delta S = \frac{2(I_s - I_p)}{I_s + I_p} \approx 2.3\Gamma\varepsilon = 2.3\mathrm{A} \quad (1)$$

where Γ is the surface concentration of the adsorbed species and ε is the decimal molar absorption coefficient of the adsorbed species.

3. Results and discussion

3.1. Electrochemistry

The spreading of SUVs onto the gold electrode surface can be conveniently studied by recording differential capacity of the interface. These measurements provide useful information concerning the compactness of the film and the potential window within which the vesicles fuse onto the electrode surface. Fig. 2 shows the differential capacity curves determined for the Au(111) electrode in the 0.1M NaF solution without and with the presence of DOPC and DMPC vesicles.

In the presence of the phospholipids the differential capacity curves display a "pit" at $E > -0.5$ V, indicating that the vesicles fuse onto the electrode surface. Independent

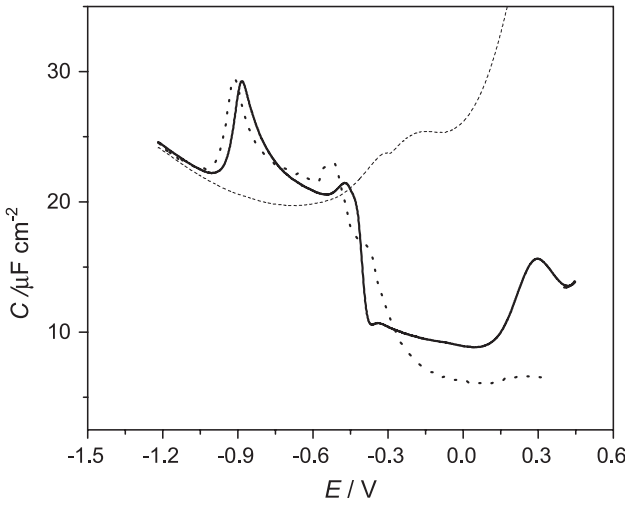

Fig. 2. The differential capacity–potential plots for (solid line) DMPC and (dotted line) DOPC vesicles spreading on Au(111) surface in 0.05 M NaF solution, $v = 5$ mV s^{-1}, $A = 5$ mV, $f = 25$ Hz; dashed line—curve recorded in the absence of the vesicles. Potentials measured vs. a silver-silver chloride-saturated KCl electrode (SSCE).

neutron reflectivity experiments performed in our laboratory indicate that a bilayer of the phospholipids molecules is formed at these potentials [26]. However, the minimum value of the capacity corresponds to 8.5 ± 0.5 μF cm^{-2} in the presence of DMPC and 5.5 ± 0.5 μF cm^{-2} for DOPC. These numbers are much higher than the value of the capacity for a defect free bilayer of these phospholipids, expected to be equal to ~ 0.8 μF cm^{-2} [2,16]. This behavior indicates that the bilayer is not perfect and consists of rafts separated by cracks filled with the solvent. Such defected bilayers are frequently formed when vesicles fuse onto a solid support surface [9,34].

At $E < -0.5$ V (SSCE) the capacity of the electrode initially covered by the bilayer increases, indicating that the bilayer is detached from the electrode surface. The detachment progresses gradually when potential is moved in the negative direction and is completed at $E \approx -1.0$ V (SSCE). The neutron reflectivity experiments demonstrated that the bilayer remains in the close proximity to the electrode surface at these negative potentials being separated from the gold surface by a $\sim$ 1-nm-thick layer of the electrolyte [26].

Fig. 3A shows charge density curves determined from chronocoulometric experiments. The results indicate that the vesicles spread at the gold electrode surface when -10 μC cm$^{-2} < \sigma_M < 5$ μC cm^{-2} and that the bilayer is detached from the gold surface at $\sigma_M < -20$ μC cm^{-2}. Integration of the charge density curves for the phospholipid-free and the bilayer covered electrode gives the surface pressure of the film at the electrode|solution interface [35]. Fig. 3B shows the surface pressure vs. potential plots for DOPC and DMPC bilayers at the Au(111) electrode. The surface pressure curves are bell-shaped, indicating a quasi-quadratic dependence of the Gibbs energy of film formation on the

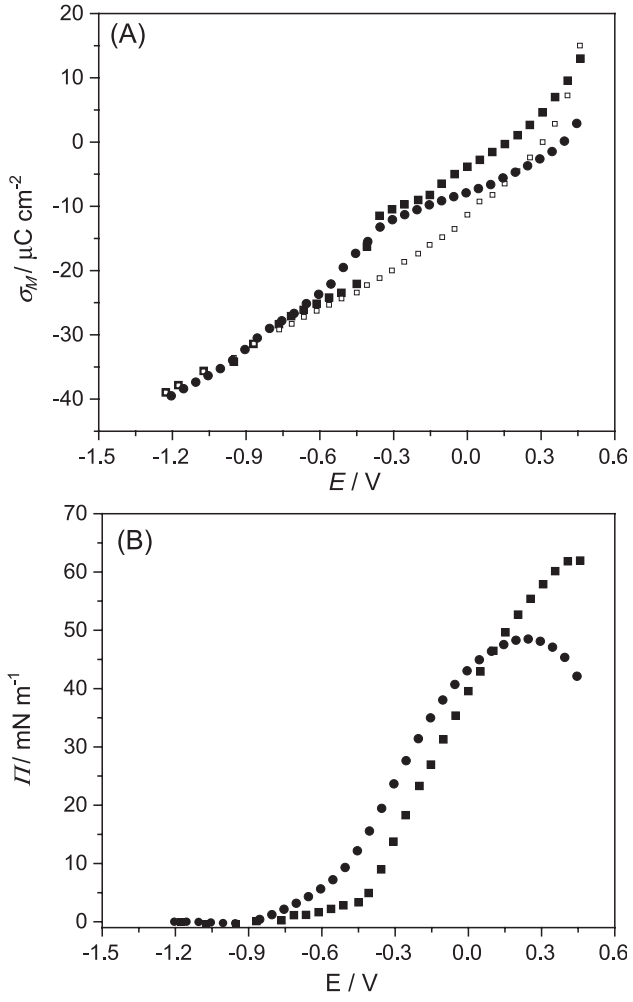

Fig. 3. (A) Charge density vs. potential curves for a Au(111) electrode in 0.05 M NaF solution. (B) Surface pressure vs. potential plots calculated from the charge density data. Open squares—supporting electrolyte, closed circles—with addition of $\sim 1\times10^{-4}$ DOPC and closed squares—in the presence of $\sim 1\times10^{-4}$ DMPC.

electrode potential. The maximum value of the surface pressure is equal to 62.0 and 48.5 mN m^{-1} for DMPC and DOPC bilayers, respectively. The equilibrium spreading pressures of the films of DMPC and DOPC formed at the gas–solution interface of an aqueous solution of vesicles are 56 and 52 mN m^{-1}, respectively. Clearly, the film pressures at the metal–solution and the gas–solution interfaces have a comparable magnitude.

The potential of the maximum surface pressure E_{max} is equal to +0.43 V (SSCE) for the DMPC bilayer, whereas for the bilayer of DOPC it is equal to +0.22V (SSCE). The potential of zero charge of the Au(111) electrode is equal to 0.31V (SSCE). For DMPC the E_{max} is positively shifted with respect to pzc. For DOPC this shift is negative. These differences suggest a different orientation of the zwitterionic head groups in the bilayers of DMPC and DOPC and/or some asymmetry between both leaflets of the bilayer obtained from the vesicles, which are known to show some asymmetry on both layers [19,20]. Overall, the electrochemical behaviour of films formed by fusion of DMPC and DOPC vesicles at the Au(111) electrode surface are quite similar. However, there are apparent differences between the behaviour of these films. They are most likely caused by the different physical state of these films, the gel state for DMPC and the liquid crystalline state for DOPC. Below we employ the PM-IRRAS technique to investigate the physical state of the two bilayers formed at the electrode surface.

3.2. Spectroelectrochemistry

The IR spectra in the CH stretching region of phospholipids contain valuable information concerning the conformation and orientation of the acyl chains and the physical state of the bilayer. Fig. 4A and B shows PM FTIRRA spectra in the CH stretching region for DMPC and DOPC

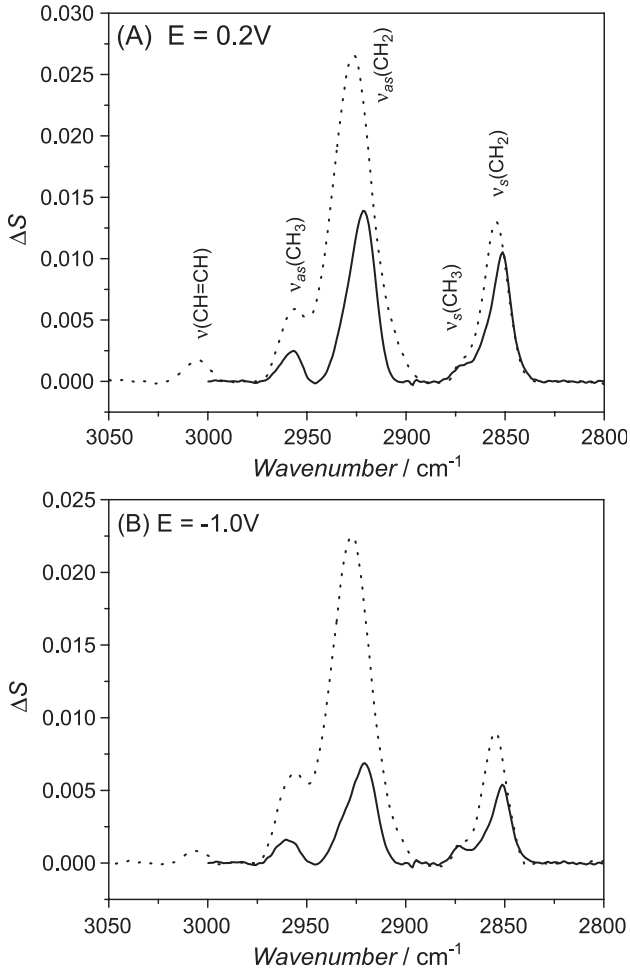

Fig. 4. The PM FTIRRA spectra in CH stretching region for bilayers of DMPC (solid line) and DOPC (dotted line) at the Au(111) electrode surface for $E=0.2$ V (SSCE) [panel (A)] and $E=-1.0$ V (SSCE) [panel (B)] in 0.05 M NaF/D_2O and $\sim 1\times10^{-4}$ M solution of the phospholipids.

bilayers at the Au(111) electrode surface, for two selected potentials 0.2 and −1.0 V (SSCE), respectively. The CH stretch region consists of four bands corresponding to the asymmetric $\nu_{as}(CH_3)$ located at ~2955 cm^{-1} and $\nu_{as}(CH_2)$ at ~2920 cm^{-1} and the symmetric stretches $\nu_s(CH_3)$ at ~2870 cm^{-1} and $\nu_s(CH_2)$ at ~2850 cm^{-1} [36,37]. In addition, the spectrum for DOPC shows a small band corresponding to the CH stretch of the unsaturated oleoyl group located at ~3006 cm^{-1} [37]. Clearly, the amplitude of these bands and band positions depend strongly on the nature of the phospholipid molecule and the applied potential.

Fig. 5A and B plots frequencies of the asymmetric (panel A) and the symmetric (panel B) CH_2 stretches as a function of the applied potential. The band frequencies

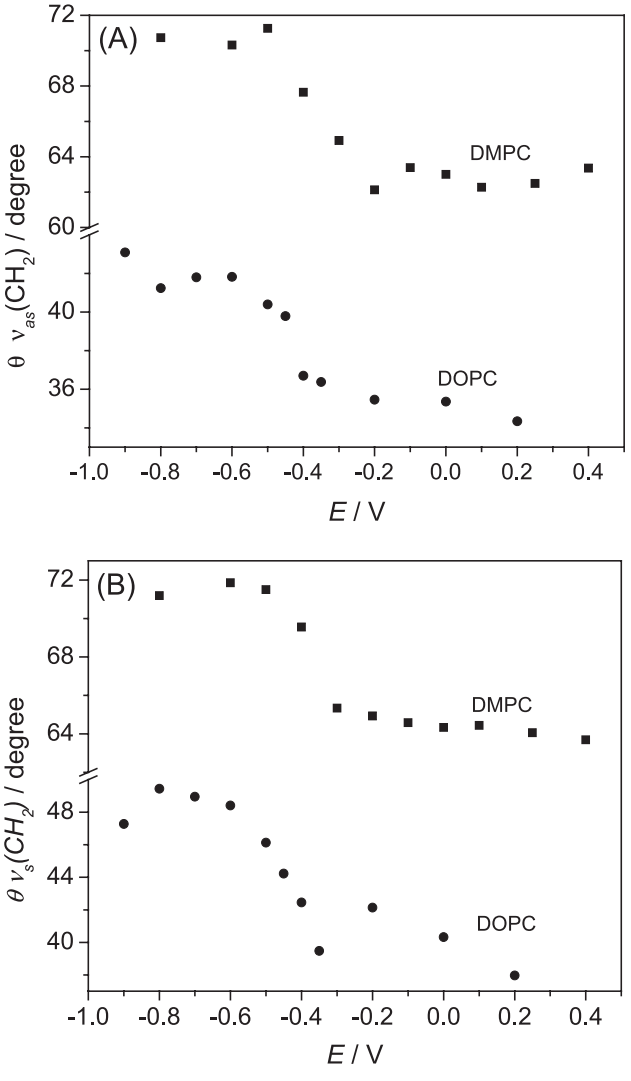

Fig. 5. The dependence of the band position on the electrode potential (A) for the asymmetric CH_2 stretch and (B) the symmetric CH_2 stretch; closed circles—DOPC, closed squares—DMPC in 0.1 M NaF/D_2O and ~1×10^{-4}M solution of the phospholipids. Potentials measured vs. a silver-silver chloride-saturated KCl electrode (SSCE).

for the film formed by DOPC are about 4 to 9 cm^{-1} shifted to higher frequencies in comparison to the position of the corresponding bands in the bilayer of DMPC. The positions of CH_2 stretch bands are known to be sensitive to conformational changes of the acyl chains [36,38,39]. The frequencies equal or lower than 2920 cm^{-1} for the asymmetric and 2849 cm^{-1} for the symmetric methylene stretch are characteristic for the all trans conformation of the acyl chains observed in the gel state [39,40]. Higher frequencies indicate presence of gauche conformations and melting of the chains [38,40].

The frequencies of methylene stretches in the film of DOPC are ~2928 cm^{-1} for the asymmetric stretch and ~2855 cm^{-1} for the symmetric methylene stretch. These values indicate that the film is in the liquid crystalline state [37,38]. The frequencies of the asymmetric and symmetric CH_2 stretches in the film of DMPC are ~2920 and 2851 cm^{-1}, respectively. These numbers suggest that the film consists of a mixture of all-trans and partially melted chains with gauche conformations. At temperature ~20 °C, multilayers of DMPC are known to form the so-called ripple phase which results from the segregation of the well ordered all trans chains and partially melted chains into ordered domains [41]. The frequencies of the CH_2 bands in the film of DMPC at the Au(111) electrode surface are consistent with this structure of the bilayer.

Further information concerning the order in the films of phospholipids deposited at the electrode surface can be extracted from the analysis of the half-widths of the absorption bands. For the film formed by DMPC, the half-width of the $\nu_{as}(CH_2)$ peak is 10.6 ± 0.2 cm^{-1}. In the spectrum of a vesicles dispersion (not shown here) the half width is equal to 12.4 cm^{-1}. The half-width of the symmetric methylene stretch is equal to 8.4 ± 0.2 cm^{-1} in the film and to 11.0 cm^{-1} in the vesicles solution. Since more ordered films have narrower IR bands, these results indicate that the bilayer of DMPC deposited at the Au(111) electrode surface is more ordered than the bilayer in the aqueous dispersion of SUVs.

In the film of DOPC deposited at the gold surface the half-width of the asymmetric peak is equal to 20.6 ± 0.3 cm^{-1} and is comparable to that in a vesicles dispersion −21.4 cm^{-1}. The half-width of $\nu_s(CH_2)$ in the film is 12.0 ± 0.2 cm^{-1} and is only slightly smaller that 13.5 cm^{-1} measured for the solution of vesicles. The half-widths of the methylene peaks are much smaller in the film of DMPC than in the bilayers of DOPC, showing lower mobility of the molecules in the bilayer.

Fig. 5A and B also shows that positions of $\nu_{as}(CH_2)$ and $\nu_s(CH_2)$ bands display weak but measurable dependence on the electrode potential. The changes correlate well with properties of these films described earlier with the help of differential capacity or charge density curves. Interestingly, positions of these bands shift with potential in the opposite direction for the two phospholipids. In the

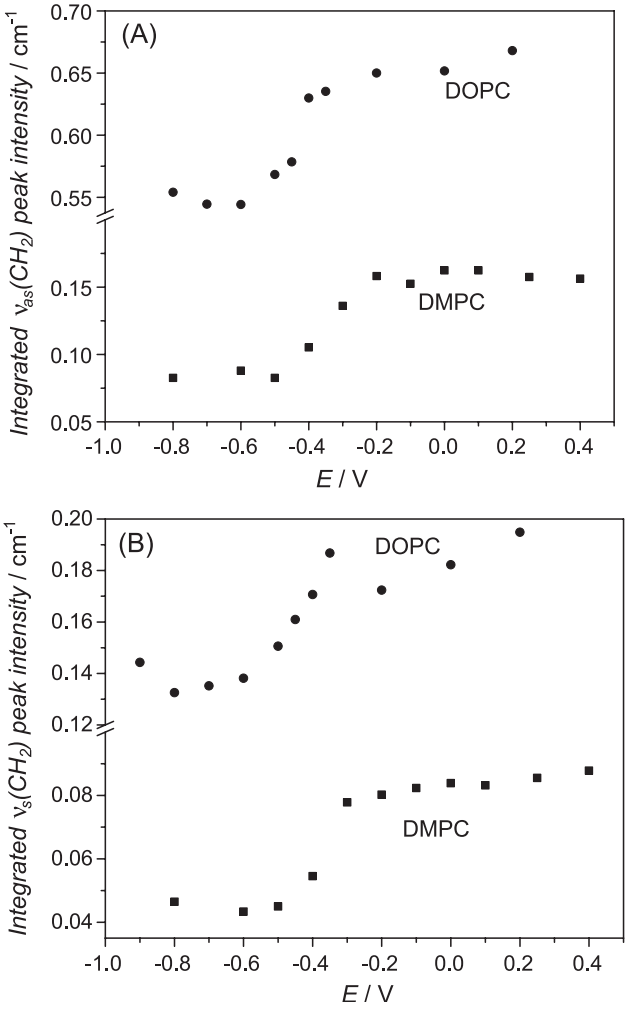

Fig. 6. The dependence of the integrated peak intensity on the electrode potential (A) for the asymmetric CH_2 stretch and (B) the symmetric CH_2 stretch; closed circles—DOPC, closed squares—DMPC in 0.1 M NaF/D_2O and $\sim 1\times10^{-4}$M solution of the phospholipids. Potentials measured vs. a silver-silver chloride-saturated KCl electrode (SSCE).

film of DMPC, the frequencies of methylene bands are somewhat higher when the bilayer is deposited directly onto the gold surface at $E>-0.5$ V (SSCE) than when the film is detached from the electrode at more negative potentials. This behaviour suggests that adsorption of the bilayer at the gold surface induces gauche conformations in the acyl chains and causes an additional melting of the chains. In contrast, in the film of DOPC the bands shift to slightly lower frequencies, indicating that adsorption of the bilayer at the metal surface results in a somewhat better ordering of the acyl chains.

Fig. 6A and B shows dependence of integrated intensities of the methylene stretching bands on the electrode potential. The intensities increase when $E>-0.5$ V (SSCE). The potential range where the intensity increases corresponds to the potential range where the differential capacity decreases and the bilayer is adsorbed onto the gold surface.

The integrated band intensity is proportional to the dot product between the transition dipole moment vector $(\vec{\mu})$ and electric filed vector $(\vec{E})$ [42]:

$$\int Adv \propto |\mu\cdot E|^2 \propto |\mu|^2\langle E^2\rangle\cos^2\theta \tag{2}$$

with θ being the angle between the direction of the transition dipole and the electric field of the photon (which is normal to the surface). Assuming that the absolute value of the transition dipole does not depend on potential, the changes of the band intensity may be interpreted as a change of the angle θ, caused by a reorientation of acyl chains of phospholipid molecules. This approximation is widely used in the IR studies of field-driven transformations in thin films at electrode surfaces [30].

We have demonstrated recently [19,20,23] that the angle θ can be calculated if the intensity of a hypothetical film consisting of randomly oriented molecules can be determined from an independent experiment. Knowing the band intensity for a film of randomly oriented molecules, the tilt angle θ can then be calculated using the formula [43,44]:

$$\cos^2\theta = \frac{1}{3}\frac{\int A_{(E)}dv}{\int A_{(random)}dv} \tag{3}$$

where $A_{(E)}$ and $A_{(random)}$ are absorbances of the IR bands for the bilayer at the electrode surface and for the hypothetical bilayer consisting of randomly oriented molecules.

Fig. 7A and B plots angles between the direction of the transition dipole of the asymmetric and symmetric methylene stretches and the surface normal, calculated from the integrated band intensities with the help of Eq. (3). The details of these calculations are described in our earlier publications [19,20]. Cartoons attached to these figures show positions of the transition dipoles with respect to the acyl chain of the phospholipids molecule. The transition dipoles of the two stretches are located in the plane of the methylene group. The transition dipole of the symmetric stretch is oriented along the group diagonal. The transition dipole of the asymmetric stretch forms a 90° with the diagonal and is aligned along the direction joining the two hydrogen atoms of this group [36,45].

The results show that the angle between directions of transition dipoles of the two CH_2 stretches and the surface normal decreases when $E>-0.5$V (SSCE). This behaviour suggests that acyl chains of DOPC and DMPC molecules are more tilted when their bilayer is directly adsorbed at the gold electrode surface. The acyl chains of the DMPC molecules are predominantly in the trans conformation. In this case, the transition dipole moments of the two methylene stretches are not only perpendicular to each other but are also perpendicular to the line of the

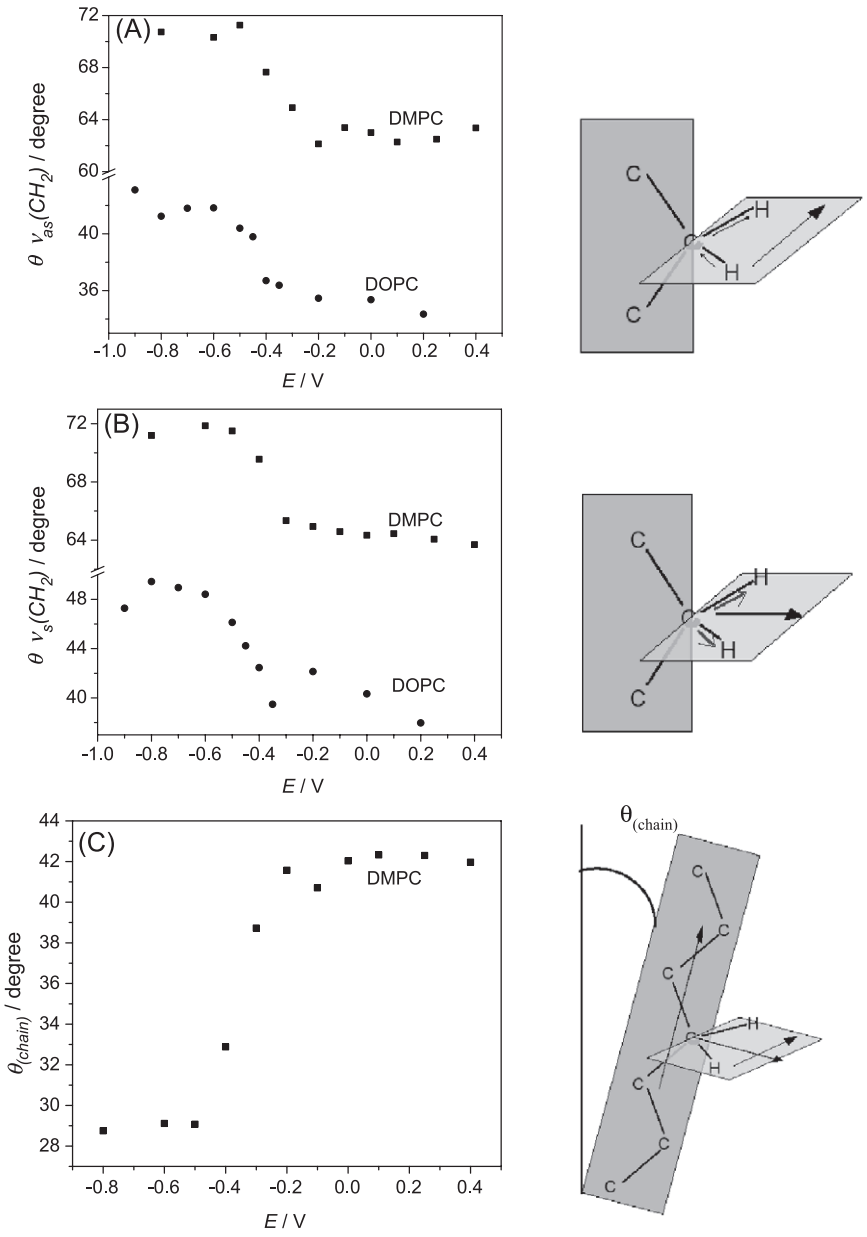

Fig. 7. The dependence of the angle (θ) between the direction of the transition dipole moment and the surface normal on the electrode potential (A) for the asymmetric CH_2 stretch and (B) the symmetric CH_2 stretch; closed circles—DOPC, closed squares—DMPC. Panel C shows the dependence of the tilt angle of the acyl chains of the DMPC molecule on the electrode potential. The experiments were carried out in 0.1 M NaF/D_2O and $\sim 1\times10^{-4}$M solution of the phospholipids. Potentials were measured vs. a silver-silver chloride-saturated KCl electrode (SSCE). Cartoons show the directions of the transition dipoles and the direction of the acyl chain.

hydrocarbon chain and the following relation must be satisfied [46]:

$$\cos^2(\theta_{vas}) + \cos^2(\theta_{vs}) + \cos^2(\text{chain}) = 1. \quad (4)$$

Eq. (4) may be used to calculate the chain tilt angle. Fig. 7C plots the chain tilt angle as a function of the applied potential. At $E < -0.5$ V (SSCE), where the bilayer is detached from the metal and according to recent neutron reflectivity data [26] is suspended on a thin cushion of the solvent, the tilt angle is equal to 29°. Comparable values of the chain tilt angle have been determined for ordered multilayers of DMPC by the X-ray diffraction technique [47,48]. The tilt angle apparently increases to 42° at $E > -0.2$ V (SSCE) where the bilayer is adsorbed at the electrode surface.

Additional information concerning the orientation of the acyl chains of the phospholipids molecules may be extracted from the integrated intensity of the symmetric methyl stretch observed at ~ 2870 cm^{-1}. This band is small and overlaps

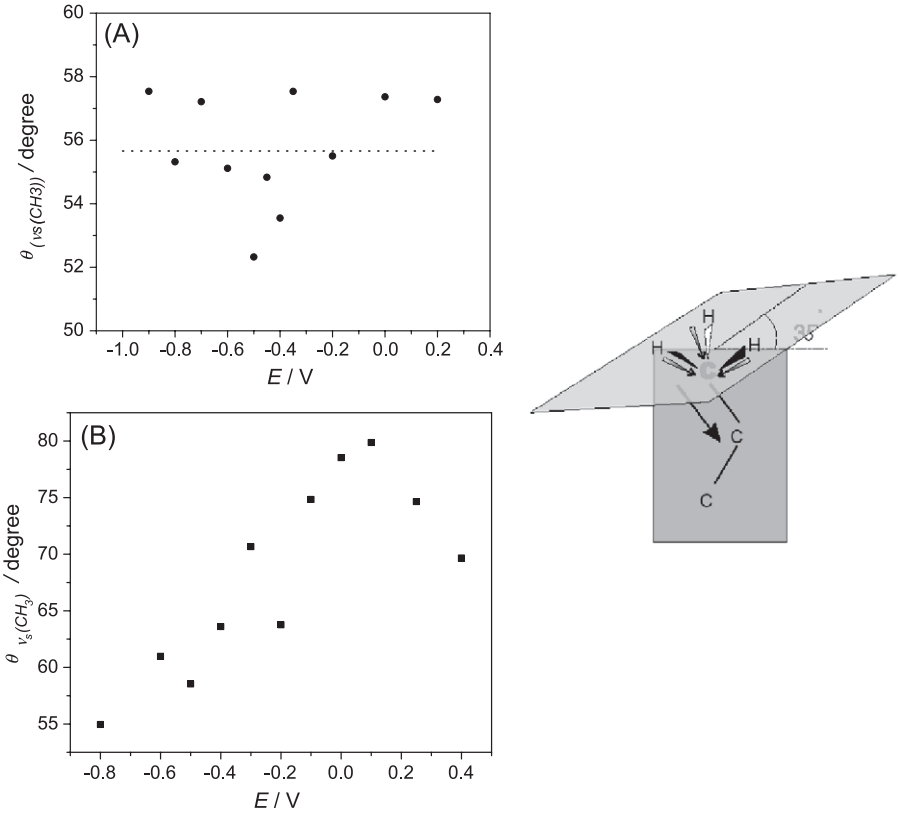

Fig. 8. The dependence of the angle (θ) between the direction of the transition dipole moment and the surface normal on the electrode potential for the symmetric CH_3 stretch, A—for DOPC and B—for DMPC. The experiments were carried out in 0.1 M NaF/D_2O and $\sim 1\times10^{-4}$M solution of the phospholipids. Potentials were measured vs. a silver-silver chloride-saturated KCl electrode (SSCE). Cartoon shows the direction of the transition dipoles of the symmetric CH_3 stretch.

with much larger band of the symmetric methylene stretch. Its analysis requires a deconvolution of this spectral region described in detail in [19,20]. Fig. 8A and B shows the dependence of the angle between directions of the transition dipole of this band and the surface normal. The position of the transition dipole with respect to the direction of the acyl chain is shown in the cartoon attached to Fig. 8. The transition dipole is oriented along the direction of the C–C bond between the two terminal carbon atoms in the acyl chain [49].

As mentioned above, a deconvolution procedure has to be applied to calculate the $\nu_s(CH_3)$ band intensity. Therefore, the uncertainty of the calculated values is quaite large. Nevertheless, the data in Fig. 8 show that for the film of DOPC the angle is independent of the applied potential and its values are scattered around 55°. This result indicates that directions of the bond between the last two carbon atoms in the acyl chain are distributed randomly and hence that the film is disordered. In contrast, for the film of DMPC the angle increases with the electrode potential. A simple geometrical analysis tells that the direction of the transition dipole of the $\nu_s(CH_3)$ band forms a $\sim 35°$ angle with the direction of the fully extended all-trans acyl chain. Subtracting this number from the data shown in Fig. 8B, one gets the chain tilt angles ranging from 20° at negative to 45° at positive potentials, in a reasonable agreement with the result of the analysis of the methylene bands and presented in Fig. 7C. Apparently, consistent information can be extracted from the analysis of different bands in the IR spectrum.

4. Summary and conclusions

We have compared spreading of SUVs of DMPC and DOPC at the Au(111) electrode surface. Differential capacity and charge density curves demonstrated that the vesicles spread onto the gold surface at $E > -0.5$ V (SSCE). The films formed by DOPC and DMPC displayed a somewhat different behaviour. The PM-IRRAS has been employed to investigate the physical state of films formed at the electrode surface by the phospholipids. The analysis of CH stretching region of the IR spectra of these molecules revealed that the film formed by DOPC is in the liquid crystalline state while the film formed by DMPC is in the gel or in the ripple phase state.

The IR studies demonstrated that adsorption of the phospholipids onto the metal surface results in a significant change of the tilt of acyl chains with respect to the surface

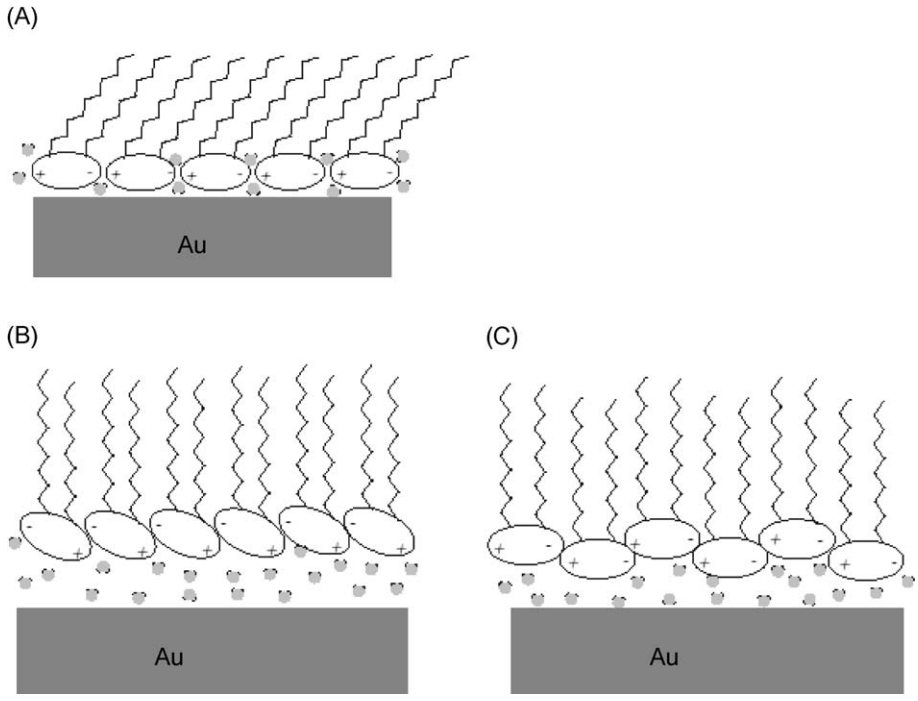

Fig. 9. Schematic representation of packing of the DMPC molecules, at (A) $E > -0.5$ V, where the bilayer is directly adsorbed at the metal surface and at (B, C) $E < -0.5$ V (SSCE), where the bilayer is suspended on a cushion of solvent.

normal. In the bilayer formed by DMPC, the acyl chains are tilted by $\sim 29°$ with respect to the surface normal at negative potentials where the film is detached and separated from the metal by a thin layer of the solvent. In the film directly adsorbed at the metal surface the tilt angle increases to $\sim 42°$.

The change in the tilt of hydrocarbon chains indicates that the area per phospholipd molecule in the bilayer (A) changes as well. The tilt angle of the chain $\theta_{(\text{chain})}$ and the area per molecule A are related by the formula [48,49]:

$$A\cos\theta_{\text{chain}} = n\Sigma \tag{5}$$

where Σ is the cross sectional area of the chain and n is the number of chains in the molecule. For DMPC $n\Sigma = 0.38$ nm^2 [47] and the tilt angle data indicate that the area per DMPC molecule in the bilayer changes from ~ 0.43 nm^2 at negative potentials, where the bilayer is separated from the metal by a thin cushion of the solvent, to ~ 0.51 nm^2 at $E > -0.5$ V (SSCE), where the film is adsorbed at the gold surface.

A plausible explanation of this change of the area per molecule may be given in terms of a change in the packing of the polar heads. According to Hauser et al. [48], phospholipids pack with a parallel arrangement of the phosphoryl-choline group as schematically shown in Fig. 9A, when the areas per molecule are in the range of 0.47 to 0.54 nm^2. For smaller areas per molecule, a tilted or zig-zag arrangement of the phosphoryl-choline group is expected, as shown by cartoons 9B and 9C, respectively. Our data indicate that model 9A describes structure of the bilayer adsorbed at the metal surface at $E > -0.5$ V (SSCE) where indeed all polar heads tend to interact with the metal. At more negative potentials, where bilayer is detached from the metal and suspended on a cushion of the solvent, the area per molecule is consistent with either a tilted or zig-zag packing of the phosphoryl-choline groups observed in hydrated multilayers of phospholipids.

In conclusion, we have demonstrated that a combination of electrochemical measurements with PM IRRAS experiments allows one to describe spreading of vesicles at a metal electrode surface and to provide detailed information concerning the structure and physical state of the film and the orientation and conformation of the phospholipid molecules in the film at the metal–solution interface.

Acknowledgements

This work was funded by an NSERC research grant. JL would like to acknowledge the Canadian Foundation for Innovation (CFI) for a Canadian Research Chair Award.

References

[1] G. Roberts (Ed.), Langmuir–Blodgett Films, Plenum, New York, 1990, chapter 6, pp. 273–307.
[2] R. Guidelli, G. Aloisi, L. Beccuci, A. Dolfi, M.R. Moncelli, F. Tadini Buoninsegni, J. Electroanal. Chem. 504 (2001) 1.

[3] D.M. Tiede, Biochim. Biophys. Acta 811 (1985) 357.
[4] C. Yuan, J. Furlong, P. Burgos, L.J. Johnston, Biophys. J. 82 (2002) 2526.
[5] H. Lang, C. Duschl, H. Vogel, Langmuir 10 (1994) 197.
[6] E. Sackmann, Science 271 (1996) 43.
[7] S. Lingler, I. Rubinstein, W. Knoll, A. Offenhausser, Langmuir 13 (1997) 7085.
[8] V. Stauffer, R. Stoody, J.O. Agak, D. Bizzotto, J. Electroanal. Chem. 516 (2000) 73.
[9] Z.V. Leonenko, A. Carnini, D.T. Cramb, Biochim. Biophys. Acta 1509 (2000) 131–147.
[10] C.W. Meuse, G. Niaura, M.M.L. Lewis, A.L. Plant, Langmuir 14 (1998) 1604.
[11] C.W. Meuses, S. Krueger, C.F. Majkrzak, J.A. Dura, J. Fu, J.T. Connor, A.L. Plant, Biophys. J. 74 (1998) 1388.
[12] R. Naumann, S.M. Schiller, F. Giess, B. Grohe, K.B. Hartman, I. Karcher, I. Koper, J. Lubben, K. Vasilev, W. Knoll, Langmuir 19 (2003) 5435–5443.
[13] A. Nelson, A. Benton, J. Electroanal. Chem. 202 (1986) 253.
[14] D. Bizzotto, A. Nelson, Langmuir 14 (1998) 6269.
[15] D. Bizzotto, V. Zamlynny, I. Burgess, C.A. Jeffrey, H.Q. Li, J. Rubinstein, Z. Galus, A. Nelson, B. Pettinger, A.R. Merill, J. Lipkowski, Amphiphilic and ionic surfactants at electrode surfaces, in: A. Wieckowski (Ed.), Interfacial Electrochemistry, Theory, Experiment and Applications, Marcel Dekker, New York, 1999, pp. 405–426.
[16] F. Tadini Buoninsegni, R. Herrero, M.R. Moncelli, J. Electroanal. Chem. 452 (1998) 33.
[17] A.L. Plant, Langmuir 9 (1993) 2764.
[18] S.L. Horsewell, V. Zamlynny, H.Q. Li, A.R. Merrill, J. Lipkowski, Faraday Discuss. 121 (2002) 405.
[19] I. Zawisza, A. Lachenwitzer, V. Zamlynny, S.L. Horswell, J.D. Goddard, J. Lipkowski, Biophys. J. 85 (2003) 4055–4075.
[20] X. Bin, J. Lipkowski, Biochemistry (in preparation).
[21] P. Krysinski, A. Zebrowska, A. Michota, J. Bukowska, L. Becucci, M.R. Moncelli, Langmuir 17 (2001) 3852.
[22] T.Y. Tsong, R.D. Astumian, Annu. Rev. Physiol. 50 (1988) 273.
[23] V. Zamlynny, I. Zawisza, J. Lipkowski, Langmuir 19 (2003) 134.
[24] J. Israelachvili, "Physics of amphiphiles: micelles, vesicles and microemulsions", in: V. DeGiorgio, M. Corti, (Ed.) Elsevier, New York, 1997, p. 24.
[25] H.L. Casal, H.H. Mantsch, Biochim. Biophys. Acta 779 (1984) 381.
[26] I. Burgess, G. Szymanski, M. Li, S. Horswell, J. Lipkowski, J. Majewski, S. Satija, Biophys. J. 86 (2004) (in print).
[27] Y. Barenholz, D. Gibbes, B.J. Litman, J. Goll, T.E. Thompson, R.D. Carlson, Biochemistry 16 (1977) 2806.
[28] D. Dickertmann, J.W. Schultze, F.D. Koppitz, Electrochim. Acta 21 (1976) 967.
[29] J. Richer, J. Lipkowski, J. Electrochem. Soc. 133 (1985) 121.
[30] N. Li, V. Zamlynny, J. Lipkowski, F. Henglein, B. Pettinger, J. Electroanal. Chem. 524/525 (2002) 43.
[31] M.J. Green, B.J. Barner, R.M. Corn, Rev. Sci. Instrum. 62 (1991) 1426.
[32] B.J. Barner, M.J. Green, E.I. Saez, R.M. Corn, Ann. Chem. 63 (1991) 55.
[33] T. Buffeteau, B. Desbat, D. Blaudez, J. Turlet, Appl. Spectrosc. 54 (2000) 1646.
[34] C. Yuan, L.J. Johnston, Biophys. J. 81 (2001) 1059.
[35] J. Lipkowski, L. Stolberg, in: J. Lipkowski, R.N. Ross (Eds.), Adsorption of Molecules at Metal Electrodes, VCH Publishers, New York, 1985, p. 171, Chp. 4, 1992.
[36] R.G. Snayder, S.L. Hsu, S. Krimm, Spectrochim. Acta 34A (1978) 395.
[37] U.P. Fringeli, Z. Naturforsch. 32C (1977) 20.
[38] R.G. Snyder, H.L. Strauss, C.A. Elliger, J. Phys. Chem. 86 (1982) 5145.
[39] R.A. MacPhail, H.L. Strauss, R.G. Snyder, C.A. Elliger, J. Phys. Chem. 88 (1984) 334.
[40] H.L. Casal, H.H. Mantsch, Biochim. Biophys. Acta 779 (1984) 381.
[41] T. Heimburg, Biophys. J. 78 (2000) 1154.
[42] M. Moskowits, J. Chem. Phys. 77 (1982) 4408.
[43] D.L. Allara, A. Baca, C.A. Pryde, Macromolecules 11 (1978) 1215.
[44] D.L. Allara, J.D. Swalen, J. Phys. Chem. 86 (1982) 2700.
[45] P.A. Chollet, J. Messier, C. Rosilio, J. Chem. Phys. 64 (1976) 1042.
[46] J. Umemura, T. Kamata, T. Kawai, T. Takenaka, J. Phys. Chem. 94 (1990) 62.
[47] M.J. Janiak, D.M. Small, G.G. Shipley, J. Biol. Chem. 254 (1979) 6068.
[48] H. Hauser, I. Pascher, R.H. Pearson, S. Sundell, Biochim. Biophys. Acta 650 (1981) 21.
[49] J.F. Rablot, F.C. Burns, N.E. Schlotter, J.D. Swalen, J. Chem. Phys. 78 (1983) 946.